RAD Conference Proceedings, vol. 7, pp. 28-33, 2023
ISSN 2466-4626 (online) | DOI: 10.21175/RadProc.2023.06
www.rad-proceedings.org

ENVIRONMENTAL MICRODOSIMETRY IN VERY LOW DOSE RATE RADIATION FIELDS

Gabriele Auriemma[1,2], Anna Bianchi[2], Anna Selva[2], Valeria Conte[*,2]

[1]Politecnico di Milano, dipartimento di Energia, via La Masa 34, 20156 Milano, Italy
[2]Laboratori Nazionali di Legnaro – INFN, Viale dell'università 2, 35020 Legnaro (PD), Italy

Abstract. *Low-dose radiation (LDR) has been demonstrated to have a significant impact on various immune response mechanisms, potentially eliciting both stimulatory and adaptive reactions within living organisms. The precise cellular mechanisms responsible for these radiation-induced immune responses warrant further in-depth investigation. Within this context, the presence of research facilities both underground and at ground level at the Gran Sasso Laboratories of the Italian National Institute of Nuclear Physics (INFN-LNGS) presents an excellent opportunity for exploring the influence of low and extremely low doses of radiation in provoking immune responses. Conducting in vitro and in vivo studies on the effects of LDR introduces several uncertainties, including the radiation quality, which is often not closely monitored, and various uncontrolled physical variables. To address these challenges, microdosimetric techniques will be employed to continuously monitor the absorbed dose and linear energy transfer (LET) distribution of the environmental radiation field. This becomes particularly important at such low dose levels, where the process of radiation interaction is primarily governed by stochastic effects, even for low LET radiation. To facilitate this research, a large spherical tissue equivalent proportional counter (TEPC) with a diameter of 5 cm has been designed at the Legnaro National Laboratories (LNL) of INFN. It is filled with propane gas to simulate a thickness of 1-2 µm of biological tissue. This study presents and discusses microdosimetric spectra measured using the aforementioned TEPC in various experimental scenarios.*

Keywords. *Low dose radiation fields, Microdosimetry, TEPC, Environmental background*

1. INTRODUCTION

Natural background radiation (NBR) is an unavoidable abiotic factor that affects all living organisms. It combines cosmic and terrestrial radiation, and it has been a constant presence throughout the evolution of life on Earth. Its role in biological systems and evolution is still not fully understood. Since the late 1980s, experiments revealed increased proliferation in organisms shielded from radiation [1]. More recently, research in underground radiobiology has shown diverse responses to below background radiation (BBR) across various life forms, suggesting a potential role for NBR in strengthening defense mechanisms [2]. This challenges the Linear non-Threshold (LNT) model's assumptions and suggests a potential beneficial effect of NBR. DISCOVER22 (DNA Damage and Immune System Cooperation in Very Low Radiation Environment 2022) is a three-year experiment funded by the National Institute for Nuclear Physics (INFN). Studies will be conducted at INFN Gran Sasso National Laboratory (LNGS). Started in early 2023, the project explores the effects of BBR on immune responses using in vitro and in vivo models. LNGS offers ideal conditions for studying low radiation exposure effects. Within the underground laboratory, cosmic ray exposure is negligible, and the presence of thorium- and uranium-poor dolomite rocks results in an extremely low neutron flux, reduced by a factor of 10^3 compared to the Earth's surface [3]. Radon and gamma–rays are the primary sources of radiation exposure. An efficient air ventilation system keeps radon levels comparable to the surface, the gamma dose rate is about 20 nGy/h [4]. Underground radiobiology demands precise environmental control in both underground and reference labs to confidently attribute biological differences to reduced NBR. Accurate radiation field characterization is crucial for experiment optimization and result interpretation. Integrating direct microdosimetric measurements with biological analyses will yield valuable insights into interactions at ultralow doses with living organisms. The use of direct microdosimetric measurements in underground radiobiology experiments represents an innovative approach, given the traditional reliance on simulations in this field [5].

The aim of this work was to explore the application of microdosimetric techniques, by means of a Tissue-Equivalent Proportional Counter (TEPC), for the assessment of natural background radiation, even at ultra-low doses. The study was developed within a collaboration between Politecnico of Milano and Legnaro National Laboratories (LNL) of INFN. A spherical TEPC with a 5 cm internal diameter, previously developed at LNL, has been used. The TEPC was exposed to different radiation environments with varying characteristics, in terms of both intensity and composition. This research will provide valuable insights for the development of a novel TEPC intended

[*] E-mail of the corresponding author – valeria.conte@lnl.infn.it

for use in the underground setting of LNGS, where background radiation levels are extremely low.

2. Materials and Methods

Traditional dosimetry measures absorbed dose, representing the average energy deposited per unit mass by ionizing radiation in a material. However, it is vital to recognize that biological responses also hinge on the microscopic spatial distribution of energy within tissues and cells [6]. Even when two volumes receive the same absorbed dose, their microscopic energy distribution can vary considerably. Uneven patterns, typically linked to densely ionizing radiation, can exert a more significant biological impact than uniform distributions seen in sparsely ionizing radiation. This aspect becomes especially relevant at low dose levels, where many microscopic targets may remain unaffected by interaction events. Given the documented dose rate of 20 nGy/h at LNGS [4], the characterization of both the total absorbed energy and its microscopic spatial distribution within tissues and cells is essential in this unique underground environment.

2.1. Microdosimetry

Microdosimetry studies the distribution of energy deposited by ionizing radiation at the microscopic level. The fundamental quantities are defined in ICRU report number 36 [7]. The specific energy (z) is defined as:

$$z = \frac{\varepsilon}{m} \quad (1)$$

Where ε is the energy imparted by ionizing radiation to the matter of mass m.
The lineal energy (y) is defined as:

$$y = \frac{\varepsilon_1}{\bar{l}} \quad (2)$$

where ε_1 is defined as the imparted energy to the matter in a volume by a single energy-deposition event and $\bar{l}$ is the mean chord length of that volume.

Specific and lineal energies are stochastic quantities, characterized by probability distributions. The most represented distributions are mainly two: the probability density function and the probability density of absorbed dose. Specifically, the probability density function, denoted as $f(y)$, is defined such that $f(y)\mathrm{d}y$ represents the probability that an event will have a lineal energy between y and $y + \mathrm{d}y$. The probability density of absorbed dose, $d(y)$, pertains to the fraction of absorbed dose associated with events falling within the same range of lineal energy values. In other words, $d(y)\mathrm{d}y$ represents the dose fraction attributed to events with lineal energy between y and $y + \mathrm{d}y$. The mean values of the two distributions are called mean lineal energy, $\bar{y}_F$, and dose-mean lineal energy, $\bar{y}_D$, respectively:

$$\bar{y}_F = \int_0^\infty y f(y)\mathrm{d}y \quad (3)$$

$$\bar{y}_D = \int_0^\infty y d(y)\mathrm{d}y \quad (4)$$

The frequency and dose distribution of the specific energy, $f(z)$ and $d(z)$, have an analogous meaning. The direct measurement of energy imparted to microscopic biological structures, such as the cell nucleus, is not feasible yet. Therefore, replicas of these structures are used, substituting biological tissue with other materials. The most common solution is to employ a cavity of dimensions in the order of millimeters or centimeters filled with low density tissue equivalent gas, meaning it has the same chemical composition as the tissue being simulated. Two volumes are considered equivalent when ionizing particles lose the same amount of energy along their corresponding paths. Based on this, to simulate one micrometer of tissue, a larger volume filled with gas at reduced density is utilized. In the context of environmental monitoring, the spherical shape is preferred as it ensures an isotropic response. The cavity walls function as the cathode, while the central wire acts as the anode, collecting electrons. To further enhance detection sensitivity, potentially allowing us to detect single ionizations, a potential difference between the anode and cathode is set to ensure proportional mode operation. In this mode, the final electric charge is directly proportional to the initial number of ionizations caused by ionizing radiation within the sensitive volume. When the walls of the counter are constructed from material equivalent to biological tissue, usually A150 conductive plastic, it is referred to as a tissue-equivalent proportional counter (TEPC). The composition of A150 plastic is 10.1% O, 77.6% C, 3.5% N, 5.2% O, 1.7% F, and 1.8% Ca. This plastic is considered to be muscle equivalent, especially in terms of hydrogen and nitrogen content [7].

2.2. EuTEPC

The detector used in this study is a spherical TEPC, designed and constructed at Legnaro National Laboratories (LNL) and known as EuTEPC. The sensitive volume has a diameter of 5 cm [8]. It was filled with propane gas, for which a pressure of 8.2 mbar simulates 1 µm of biological tissue (ICRU muscle) [9]. The radial symmetry of the electric field, with equipotential surfaces concentrical to the central anode, is achieved by slicing the cathode in 9 segments differently biased according to their position. A drawing of the EuTEPC is given in Figure 1.

After thorough cleaning and conditioning, the detector was filled with propane gas at a pressure of 16.4 mbar, equivalent to 2 µm of simulated tissue. The cathode was biased -800 V and the anode was grounded.

2.3. Experimental set-up

A series of initial measurements took place within the thermal neutron radiation field at the MUNES facility located at LNL. Fast neutrons were generated using the 9Be(p,n)9B reaction, achieved by directing 5 MeV protons at a 60 µm thick beryllium target bonded to a vanadium substrate. The target was inclined at an angle of 72 degrees relative to the beam direction, ensuring that the 5 MeV proton beam exits the beryllium layer with a residual energy of approximately 2 MeV before stopping in the vanadium layer. This configuration maximizes neutron yield while minimizing blistering effects in the beryllium. The fast neutrons emitted from the target were then moderated within a large beam shaping assembly (BSA) comprised of heavy water and graphite, with a volume

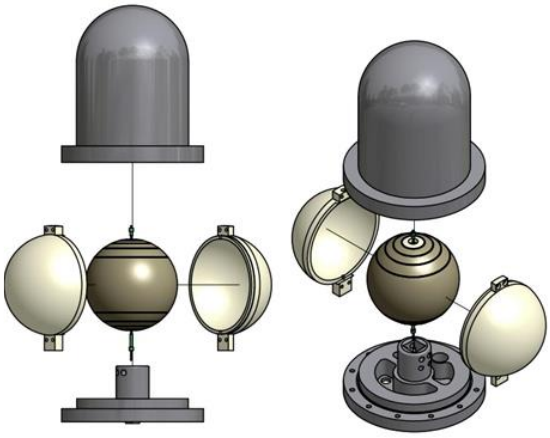

Figure 1. Drawing of the spherical EuTEPC with segmented cathode.

of about 3 m3, before being extracted through a bismuth window.

Microdosimetric measurements were conducted using the TEPC at three distinct positions surrounding the BSA, as labeled in Figure 2: A, B, and C. The distance from the right edge BSA and the detector in position A was about 1 m, from the bottom right angle and position B was about 3 m and from the bottom left angle to position C was about 3 m. The thickness of the concrete wall is 40 cm.

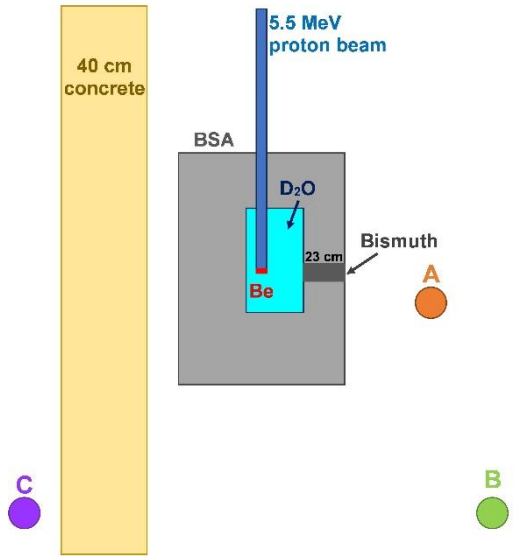

Figure 2. Schematic representation of measuring positions A, B, and C around the BSA (not to scale).

Subsequently, measurement of natural background radiation were performed in indoor environment, inside the microdosimetry laboratory of LNL, which is located at the second and last floor of the main building. Measurements were carried out during a period of reduced operational activity, when most of the machinery and accelerators were inactive. Data were recorded daily for a total duration of one week. Data analysis was performed off-line.

All spectra were calibrated on the electron-edge, setting the y_{flex}, the flex position of the Fermi-like function used to fit the electron-edge, at 7.25 keV/µm as explained in [11]. Subsequently, they were extrapolated below the noise threshold down to 0.01 keV/µm. This process involved linear fitting of experimental frequency data in a small region just above the noise level, followed by reconstructing the missing part below the noise threshold through linear extrapolation. Further details about this procedure are available in Bianchi et al.'s work [12]. We acknowledge that extrapolation is inherently uncertain, especially when the shape of the missing spectrum is unknown. However, working with spectra cut at different noise thresholds increases the uncertainty in the mean values of the distributions, $\bar{y}_F$ and $\bar{y}_D$, as discussed in [12]. Therefore, we always prefer to extrapolate the spectra, providing information on the extrapolated region. At the same time, it is our effort to keep the noise level as low as possible. Notably, the noise threshold reached with our device is already significantly lower than typical values reported in the literature, but we continue to work on improvements.

3. Results

Figures 3 and 4 provide a visual representation of the dose distributions of lineal energy, which were measured at three distinct positions surrounding the MUNES moderator, as indicated in Figure 2. In Figure 3, one can observe the distributions before undergoing calibration and extrapolation. To ensure a comprehensive and informative shape comparison, all the distributions were normalized within the pulse height range, spanning from 0.4 to 20 mV.

Upon closer examination, one initial observation becomes readily apparent: the distribution at position C stands out with more pronounced statistical fluctuations compared to the other positions. This distinctive feature is primarily attributed to the relative scarcity of data acquired at position C. While the acquisition times were roughly consistent across all positions, the fluence rate of events behind the concrete wall at position C was notably lower. Consequently, this reduced fluence rate accentuates the influence of spurious pulses originating from electron noise, notably affecting the spectrum at lower y-values. In environments characterized by extremely low background radiation levels, such challenges are to be anticipated.

Beyond statistical considerations, the shapes of the three spectra remain nearly identical up to 20 mV. This consistency suggests that, within this range, the underlying physical processes remain relatively uniform across the three positions. The contribution of larger events, stemming from interactions with neutrons, undergoes a gradual reduction as we move from position A to position C. This pattern aligns closely with the principle of increasing distance from the radiation source. This phenomenon underscores the spatial dependence of neutron interactions within the MUNES moderator, offering valuable insights into the behavior of particles within this specific environment. Understanding these interactions and their spatial distribution is pivotal for optimizing radiation monitoring and shielding strategies.

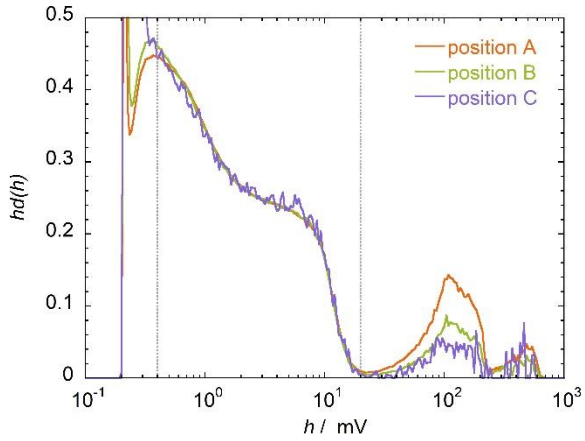

Figure 3. The uncalibrated dose-weighted distribution of the pulse height h, measured at three positions respect to the MUNES source when beam was ON (see Figure 2).

In Figure 4, the same spectra have been calibrated in terms of lineal energy and extrapolated down to 0.01 keV/µm. The $d(y)$ distributions have been normalized to a unit dose over the entire y-range, so that equal visual area under the curves correspond to

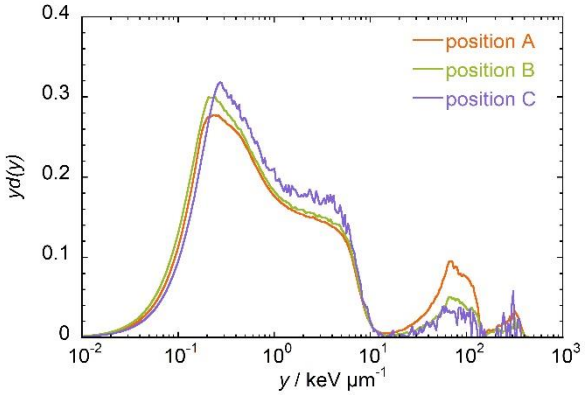

equal contributions to the total absorbed dose. At first glance, it is possible to observe that the three spectra have a similar shape, characterized by a significant contribution from events below 10 keV/µm and a smaller one from events above this threshold. The few events above 10 keV/µm can mainly be attributed to protons produced in the $^{14}N(n,p)^{14}C$ capture reaction with thermal neutrons and recoils from residual fast neutrons. In particular, the peak around 100 keV/µm is probably due primarily to the $N^{14}N(n,p)^{14}C$ reaction. In this respect, it is worth emphasizing that the nitrogen content in A150 closely aligns with that of biological tissue (muscle). The dose fraction attributed to events above 10 keV/µm gradually decreases when moving from position A to position C. To be more specific, it decreases from about 12% in position A to approximately 5% in position C, as indicated in Table 1.

Figure 4. Dose distributions of the lineal energy measured when beam was ON (see Figure 2) at three positions relative to the MUNES source. Extrapolated portions of the spectra are below 0.15 keV/µm for positions A and B, and below 0.25 keV/µm for position C.

Figure 5 depicts the spectrum measured at position A under two distinct conditions: during beam delivery (orange) and from residual activation background (red) after the accelerator shut down during the night.

Table 1. Dose fraction measured at the three positions (see Figure 2) and in position A with the beam OFF (see Figure 5). Only statistical uncertainties are reported.

	Below 10 keV/µm	Above 10 keV/µm
A	88±1%	12±1%
B	94±1%	6±1%
C	95±2%	5±2%
A - OFF	99.3±0.7%	0.7±0.7%

The first spectrum was acquired over half an hour, while the second one spanned the entire night. Obviously, the dose rate during the background measurement was considerably lower than when the beam was on target, as the counted events in the last case were exclusively due to activation and environmental radiation. The acquisition time was therefore extended to the whole night to reach significant statistics.

The shape of the spectrum below 10 keV/µm shows significant differences, in the form of a higher peak at lower lineal energy values. The increased population of this peak reflects the emission of energetic prompt gamma-rays, when the beam is active. Furthermore, the contribution of events with larger lineal energy values, occurring beyond the 10 keV/µm threshold and due to neutron interactions, vanishes when the beam is turned off.

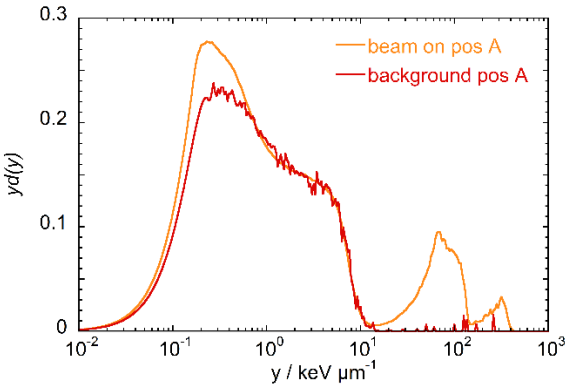

Figure 5. The microdosimetric spectrum measured in position A (see Figure 2) with proton beam ON and OFF. Extrapolated portions of the spectra are below 0.15 keV/µm for beam ON and below 0.20 keV/µm for beam OFF.

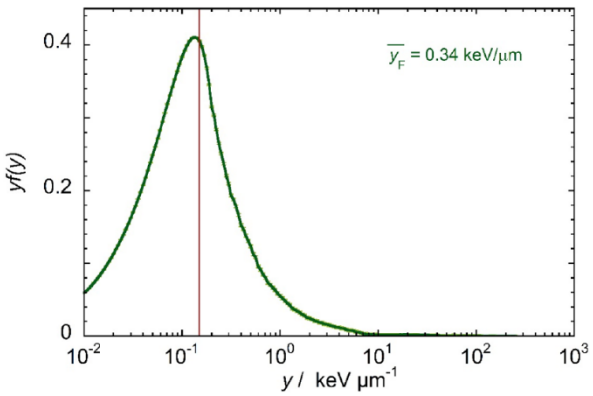

Figure 6. The frequency microdosimetric spectrum for background radiation, acquired over a week in the microdosimetry laboratory.

Figure 6 shows the frequency distribution, while Figure 7 displays the dose lineal energy distribution, both of which were measured within the background radiation field inside the microdosimetry laboratory at LNL. The vertical red line indicates the experimental detection threshold, approximately at around 0.15 keV/µm. Light green bars represent statistical uncertainties, expressed as two standard deviations. The frequency and dose mean values of the lineal energy are also reported in the figures and amount to 0.34 keV/µm and 12.8 keV/µm, respectively.

Upon observing Figure 6, it becomes evident that the frequency distribution is predominantly composed of events below 10 keV/µm. Conversely, when examining Figure 7, it becomes apparent that the dose distribution comprises two distinct components: a component of smaller events associated with the broad peak roughly below 10 keV/µm and a component of larger events spanning the range between 10 and 300 keV/µm. Although these larger events, primarily resulting from the interaction of incoming neutrons, are rare, they contribute 20% to the total dose and raise $\bar{y}_D$ to 12.8 keV/µm. The remaining 80% of the dose is attributed to small-y events, mainly arising from gamma-rays interactions with the TEPC walls.

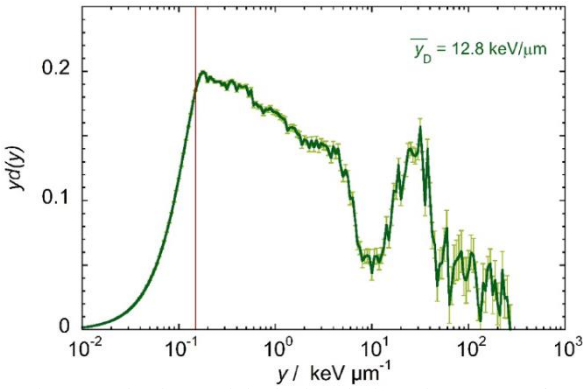

Figure 7. The dose weighed microdosimetric spectrum for background radiation acquired over a week in the microdosimetry laboratory.

The total number of events recorded in one week amounts to $2.9 \cdot 10^5$. Using the $\bar{y}_F$ value obtained from the measurement and considering the total number of events acquired over a period of 163 hours, it was possible to calculate the average dose and dose rate associate to the background radiation field: 8 µGy and 50 nGy/h, respectively. Taking into account that 80% of this dose is attributed to the small-y events, the gamma dose-rate amounts to approximately 40 nGy/h, which is roughly twice the value measured in the LNGS underground laboratory.

To verify the data consistency, Figure 8 depicts the acquired spectrum together with a distribution measured at sea level in Ottawa (Canada) with a commercial Hawk-TEPC Environmental Monitor from FarWest Technology, simulating 2 µm [13]. It is noticeable that the general shape of the two spectra is very similar. In particular, the dose fractions below and above 10 keV/µm are of the same order of magnitude.

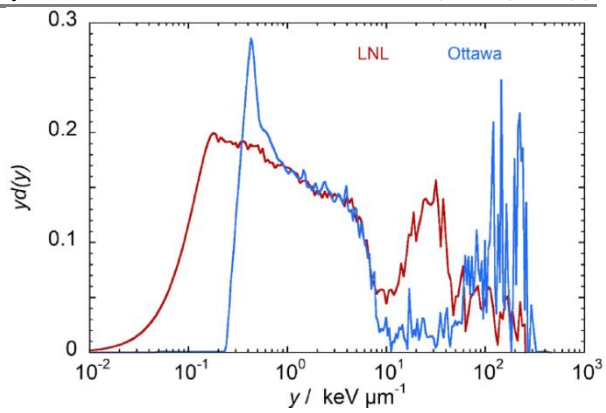

Figure 8. Comparison of the background microdosimetric spectrum measured at LNL with that measured in Ottawa. Literature data adapted from [12].

In the region above approximately 10 keV/µm, a notable difference is evident. The Legnaro spectrum displays a pronounced peak at 20-30 keV/µm, whereas in the Ottawa spectrum this peak is observed at higher lineal energy levels. This dissimilarity likely stems both from distinct responses of the two detectors and from different radiation fields. Significantly, measurements were conducted in different geographical locations and at different times, with Legnaro measurements taken indoors and Ottawa measurements taken outdoors in free air. While detailed literature data is unavailable, it is improbable that the observed differences result from variations in the response functions of the EuTEPC and the Hawk-TEPC, as previous studies have demonstrated a very similar response of the EuTEPC with the FWT spherical microdosimeter in both gamma and neutron fields [14]. Notably, the noise level in the Ottawa measurements is approximately 0.6 keV/µm, compared to our detection threshold of around 0.15 keV/µm.

5. Conclusion and Future Perspectives

This experimental work was conducted at LNL. The primary goal was to explore the applicability of microdosimetric techniques to characterize the background radiation even at very low dose levels. A 5 cm spherical TEPC, previously developed at LNL was used, at 2 µm equivalent size, as environmental radiation monitor.

The EuTEPC was exposed to the thermal neutron field available at the CN accelerator facility of LNL, with the detector at different positions surrounding the neutron-moderator. Microdosimetric spectra were acquired under two conditions: with the proton beam directed at the target and with the beam halted. In the latter scenario, the measurements were specifically designed to probe and characterize the radiation field stemming from activation processes. These measurements not only shed light on the nature of the radiation environment but also underscored a critical requirement - the imperative for substantial reduction in electric noise for precise low-frequency event measurements. This imperative is not merely a technical concern; it directly impacts the accuracy of data obtained in radiation fields characterized by

activation processes, emphasizing the pivotal role of noise reduction in ensuring the reliability of microdosimetric data in such contexts.

Lastly, Environmental background measurements were conducted at the Microdosimetry Laboratory over a total exposure period of 163 hours. The dose-weighted microdosimetric spectrum revealed two distinct dose components, one below and the other above 10 keV/µm, primarily corresponding to gamma-rays and neutrons, respectively. Neutron interactions contributed 20% to the total dose increasing the $\bar{y}_D$ to 12.8 keV/µm. This result aligns with existing literature data, particularly when considering varying experimental conditions.

The mean dose rate due to gamma-rays was approximately 40 nGy/h, which is double the value observed in the LNGS underground gallery. Based on these findings, we intend to develop a new TEPC with an internal diameter of 10 cm. This TEPC will enable the collection of comparable statistical data within a week of measurements.

***Acknowledgements*:** *This work was carried out in the framework of the DISCOVER22 project funded by the 5th scientific commission of the Italian National Institute for Nuclear Physics (INFN).*

REFERENCES

1. H. Planel, J.P. Soleilhavoup, R. Tixador, G. Richoilley, A. Conter, F. Croute, C. Caratero, Y. Gaubin, "Influence on cell proliferation of background radiation or exposure to very low, chronic gamma radiation", *Health Phys.*, **52**(2), 571-8, 1987. https://doi.org/10.1097/00004032-198705000-00007
2. P. Morciano, F. Cipressa, A. Porrazzo, G. Esposito, M.A. Tabocchini, G. Cenci, "Fruit Flies Provide New Insights in Low-Radiation Background Biology at the INFN Underground Gran Sasso National Laboratory (LNGS)", *Radiat. Res.*, **190**(3), 217-225. 2018. https://doi.org/10.1667/RR15083.1
3. A. Bettini, "Underground Laboratories", *J. Phys.: Conf. Ser.*, **120**, 082001, 2008. https://doi.org/10.1088/1742-6596/120/8/082001
4. G. Esposito, P. Anello, M. Ampollini, E. Bortolin, C. De Angelis, G. D'Imperio, V. Dini, C. Nuccetelli, M.C. Quattrini, C. Tomei, A. Ianni, M. Balata, G. Carinci, M. Chiti, O. Frasciello, G. Cenci, F. Cipressa, A. De Gregorio, A. Porrazzo, M.A. Tabocchini, L. Satta, P. Morciano, "Underground Radiobiology: A Perspective at Gran Sasso National Laboratory", *Front. Public Health*, **8**, 2020. https://doi.org/10.3389/fpubh.2020.611146
5. N. Lampe, D.G. Biron, J.M.C. Brown, S. Incerti, P. Marin, L. Maigne, D. Sarramia, H. Seznec, V. Breton, "Simulating the Impact of the Natural Radiation Background on Bacterial Systems: Implications for Very Low Radiation Biological Experiments", *Plos One,* **11**(11), 2016. https://doi.org/10.1371/journal.pone.0166364
6. G. Baiocco, S. Bartzsch, V. Conte, T. Friedrich, B. Jakob, A. Tartas, C. Villagrasa, K.M. Prise, "A matter of space: how the spatial heterogeneity in energy deposition determines the biological outcome of radiation exposure.", *Radiat. Environ. Biophys.*, **61**, 545–559, 2022. https://doi.org/10.1007/s00411-022-00989-z
7. International Commission on Radiation Units and Measurements, "Microdosimetry Report 36.", Bethesda, MD, USA, 1983.
8. D. Moro, L. De Nardo, P. Colautti, V. Conte2, T. Berger, K. Marsalek, P. Beck, S. Rollet, M. Latocha, E. Bissiato, G. Egeni, G. Donà, M. Luzik-Bhadra, A. Jaksi, M. Vuotila, E. Koivula, G. Reitz, M. Dieckmann, U. Straube, "EuTEPC - (European Tissue Equivalent Proportional Counter): A microdosimeter for the assessment of the radiation quality at the international space station", LNL-INFN Annual Report, p. 111, 2011. https://www1.lnl.infn.it/~annrep/read_ar/2011/index_contrib.htm https://www1.lnl.infn.it/~annrep/read_ar/2011/contributions/pdfs/111_B_83_B078.pdf
9. S. Chiriotti, D. Moro, P. Colautti, V. Conte, B. Grosswendt, "Equivalence of pure propane and propane te gases for microdosimetric measurements.", *Radiat. Prot. Dosimetry.*, **166**(1-4), 242-6, 2015. https://doi.org/10.1093/rpd/ncv293
10. A. Selva, L. Bellan, A. Bianchi, G. Giustiniani, P. Colautti, E. Fagotti, A. Pisent, V. Conte, "Microdosimetry of an accelerator based thermal neutron field for boron neutron capture therapy.", *Appl. Radiat. Isot.*, **182**, 110144, 2022. https://doi.org/10.1016/j.apradiso.2022.110144
11. D. Moro, S. Chiriotti, V. Conte, P. Colautti, B. Grosswendt, "Lineal calibration of a spherical TEPC", *Radiat. Prot. Dosimetry*, **166**(1-4), 233–237, 2015. https://doi.org/10.1093/rpd/ncv153
12. A. Bianchi, A. Selva, P. Colautti, A. Parisi, F. Vanhavere, B. Reniers, V. Conte, "The effect of different lower detection thresholds in microdosimetric spectra and their mean values", *Radiat. Meas.*, **146**, 106626, 2021. https://doi.org/10.1016/j.radmeas.2021.10662
13. Haiqian Ma, "Application of tissue equivalent proportional counter (TEPC) in intercalibration with nai(tl) spectrometer." Master of Science in Particle Physics at Carleton University, Ottawa, Ontario, Canada, 2021.
14. D. Moro, S. Chiriotti, "EuTEPC: measurements in gamma and neutron fields", *Radiat. Prot. Dosimetry*, **166** (1-4), 266–270, 2015. https://doi.org/10.1093/rpd/ncv154